Published July 15, 2009, doi:10.4049/jimmunol.0901131

Telomere Shortening and Oxidative Stress in Aged Macrophages Results in Impaired STAT5a Phosphorylation[1]

Carlos Sebastián,* Carmen Herrero,* Maria Serra,* Jorge Lloberas,* María A. Blasco,† and Antonio Celada[2]*

Macrophages are an essential component of both innate and adaptive immunity, and altered function of these cells with aging may play a key role in immunosenescence. To determine the effect of aging on macrophages, we produced bone marrow-derived macrophages in vitro. In these conditions, we analyzed the effect of aging on macrophages without the influence of other cell types that may be affected by aging. We showed that telomeres shorten with age in macrophages leading to a decreased GM-CSF but not M-CSF-dependent proliferation of these cells as a result of decreased phosphorylation of STAT5a. Macrophages from aged mice showed increased susceptibility to oxidants and an accumulation of intracellular reactive oxygen species. In these macrophages STAT5a oxidation was reduced, which led to the decreased phosphorylation observed. Interestingly, the same cellular defects were found in macrophages from telomerase knockout (*Terc*$^{-/-}$) mice suggesting that telomere loss is the cause for the enhanced oxidative stress, the reduced Stat5a oxidation and phosphorylation and, ultimately, for the impaired GM-CSF-dependent macrophage proliferation. *The Journal of Immunology,* **2009, 183: 0000–0000.**

Aging can be defined as the time-related deterioration of the physiological functions required for survival and fertility. Among the functions affected by aging, the immune system has been shown to be dysregulated with advancing age, thus leading to increased susceptibility to viral and bacterial infections, reactivation of latent viruses, and decreased response to vaccines (1).

Macrophages from aged humans, rats, and mice display several defects in their functional activities (2), which lead to impairment in the first line of immune defense and to a decreased capacity to contribute to the development of specific immune responses by presenting Ags to T cells and producing regulatory cytokines. Thus, these alterations of macrophage functions contribute to the impairment of the immune system during aging, a process called immunosenescence, which is associated with increased mortality and a major incidence of immune diseases and cancer in the elderly.

Telomeres are chromatin structures that cap and protect the end of chromosomes. In vertebrates, they are formed by tandem repeats of hexamer sequences (TTAGGG) that are associated with various specific proteins involved in the maintenance and regulation of telomere length (3). Telomere shortening is involved in the aging process and in the regulation of replicative lifespan (4). This age-related shortening and the observation that several premature aging syndromes are associated with short telomeres support the concept that telomere length homeostasis is a crucial determinant of human longevity. Moreover, late generations of the telomerase knockout mice, *Terc*$^{-/-}$, which show severe telomere dysfunction characterized by critically short telomeres, suffer from premature aging and various age-related diseases that affect highly proliferative tissues (5, 6). Among these, the generation and function of immune cells has been shown to be affected by telomere attrition. T, B, and NK cells show telomere shortening during aging, which is associated with impaired proliferation and function of these cells (6, 7).

In this study, we show that telomeres shorten with age in mouse macrophages. We used bone marrow-derived macrophages from young and aged mice grown and differentiated in vitro. This model allows us to analyze the effect of aging without the influence of other cell types that may be affected by this process (8). Telomere shortening is associated with impaired GM-CSF- but not M-CSF-dependent proliferation of macrophages, which is caused by a reduced phosphorylation of STAT5a. These cells also show increased intracellular levels of reactive oxygen species (ROS)[3] and an enhanced susceptibility to oxidative stress. In addition, we demonstrate that STAT5a oxidation is required for its phosphorylation and that this oxidation is reduced in macrophages from aged mice. Macrophages from *Terc*$^{-/-}$ mice, which have a similar telomere length as aged macrophages, show the same phenotype as aged macrophages. Thus, these results point to telomere shortening as the molecular determinant of some aspects of macrophage aging by modulating oxidative stress.

Materials and Methods

Reagents

Recombinant murine cytokines were purchased from Sigma-Aldrich. The Abs used were anti-STAT5a, anti-STAT5b (R&D Systems), anti-phospho-STAT5a/b Y694/Y699, anti-γ-H2AX (Ser139), GM-CSF-Rα (Upstate Biotechnology), anti-histone H1, GM-CSR-Rβ (SantaCruz Biotechnology) anti-*β-actin* (Sigma-Aldrich). Peroxidase-conjugated anti-rabbit (Jackson ImmunoResearch Laboratories) or anti-mouse (Sigma-Aldrich) were used as secondary Abs. All other chemicals were of the highest purity grade

*Institute for Research in Biomedicine and University of Barcelona, Barcelona, Spain; and †Telomeres and Telomerase Group, Molecular Oncology Program, Spanish National Cancer Centre, Madrid, Spain

Received for publication April 8, 2009. Accepted for publication June 16, 2009.

The costs of publication of this article were defrayed in part by the payment of page charges. This article must therefore be hereby marked *advertisement* in accordance with 18 U.S.C. Section 1734 solely to indicate this fact.

[1] This work was supported by a Grant from the MEC BFU 2007-63712/BMC (to A.C.).

[2] Address correspondence and reprint requests to Prof. Antonio Celada, Institute of Research in Biomedicine, Baldiri Reixac 10, Barcelona Science Park, University of Barcelona, E-08028 Barcelona, Spain. E-mail address: acelada@ub.edu

[3] Abbreviations used in this paper: ROS, reactive oxygen species; DCF-DA, dichlorofluorescin diacetate; NAC, *N*-acetylcysteine; WT, wild type.

available and were purchased from Sigma-Aldrich. Deionized water further purified with a Millipore Milli-Q system A10 was used.

Cell culture

Bone marrow-derived macrophages were isolated from young (6 wk) or aged (18–24 mo) C57BL/6 mice (Charles River Laboratories and National Institute on Aging) as described (9). Mice C57BL/6 (6 wk old) lacking the gene encoding the telomerase RNA component ($Terc^{-/-}$) were generated as described (10). Bone marrow-derived macrophages from wild type (WT) and $Terc^{-/-}$ first and third generation were used. The use of animals was approved by the Animal Research Committee of the University of Barcelona (no. 2523).

RNA extraction and real-time RT-PCR

Cells were washed twice with cold PBS, and total RNA was extracted with the EZ-RNA kit as described by the manufacturer (Biological Industries). RNA was treated with DNase (Roche) to remove contaminating DNA. For cDNA synthesis, 1 μg of total RNA and M-MLV reverse transcriptase RNase H minus, Point Mutant, oligo$(dT)_{15}$ primer and PCR nucleotide mix were used, as described by the manufacturer (Promega Corporation). Real-time PCR was performed using the power SYBR green master mix (Applied Biosystems), following the manufacturer's instructions, with the exception that the final volume was 12.5 μl of SYBR green reaction mix. Real-time monitoring of PCR amplification was performed in the ABI Prism 7900 sequence detection system (Applied Biosystems). Data were expressed as relative mRNA levels normalized to the *β-actin* expression level in each sample. The primer sequences can be obtained upon request.

Proliferation assay

Macrophage proliferation was measured by [^{3}H]thymidine incorporation as described (11). Cells were deprived of M-CSF for 16–18 h and then 10^5 cells were incubated for 24 h in complete medium in the presence of the growth factor. After this period, the medium was replaced with medium containing [^{3}H]thymidine. After an additional 6 h of incubation, the medium was removed and the cells were fixed in ice-cold 70% methanol. After three washes, cells were solubilized and radioactivity was measured. Each point was performed in triplicate, and the results are expressed as the mean ± SD. For cell counting we used a hemocytometer.

Cell cycle analysis

Cell cycle was analyzed as described (12). Cells were fixed with EtOH 95%, incubated with propidium iodide plus RNase A, and then analyzed by FACS. Cell cycle distributions were analyzed with the Multicycle program (Phoenix Flow Systems).

Protein analysis

Cells were lysed as described (13) in lysis buffer (1% Triton X-100, 10% glycerol, 50 mM HEPES (pH 7.5), 150 mM NaCl, protease inhibitors and 1 mM sodium orthovanadate). For immunoprecipitation assays, 150 μg of cell lysates were mixed with 75 μl of 20% protein A-Sepharose (Sigma-Aldrich) and 2 μl of specific Abs anti-STAT5a and STAT5b to a final volume of 500 μl. The reaction was conducted overnight at 4°C in rotation. After three washes in cold washing buffer (PBS, 1% Nonidet P-40, 2 mM sodium orthovanadate) pellets were heated to 95°C in Laemmli SDS loading buffer, and proteins were resolved by SDS-PAGE. For histone H2AX Western blot, an acid extraction of proteins was performed as described by the anti-phospho-H2AX Ab manufacturer. Briefly, cells were washed in cold PBS and lysed with lysis buffer (10 mM HEPES (pH 7.9), 1.5 mM $MgCl_2$, 10 mM KCl, 0.5 mM DTT, and 1.5 mM PMSF). Hydrochloric acid was added to a final concentration of 0.2 N, and the cell lysate was incubated on ice for 30 min. After centrifugation at 11,000 × *g* for 10 min at 4°C, supernatants were dialyzed twice against 200 ml of 0.1 M acetic acid for 1–2 h and three times against 200 ml of H_2O for 1 h, 3 h, and overnight, respectively. Detection of oxidized proteins was performed by immunoprecipitating STAT5a and STAT5b and using the OxiBlot protein oxidation detection kit (Chemicon International), which detects the carbonyl groups introduced into proteins by oxidative reactions. These carbonyl groups were derivatized to dinitrophenylhydrazone by reaction with dinitrophenylhydrazine. The dinitrophenylhydrazone-derivatized proteins were separated by SDS-PAGE followed by Western blotting.

Nuclear extract preparation and DNA-binding assay

Nuclear extracts were prepared as follows: cell pellets were washed twice with cold PBS buffer and resuspended in buffer A (10 mM HEPES, 10 mM KCl, 0.1 mM EDTA, 0.1 mM EGTA, 1 mM DTT, 0.5 mM PMSF, 0.01 mg/ml aprotinin, 0.01 mg/ml leupeptin, 0.086 mg/ml iodacetamide, 1 mM sodium orthovanadate) and incubated on ice for 15 min. Cells were lysed by adding 10% Nonidet P-40 and mixing by vortex. Nuclei were collected at the bottom of the tube by a 30-s centrifugation. After three washes with buffer A, nuclei were lysed with buffer B (20 mM HEPES, 0.4 M NaCl, 1 mM EDTA, 1 mM EGTA, 1 mM DTT, 1 mM PMSF, 5 mM sodium fluoride, 0.01 mg/ml aprotinin, 0.01 mg/ml leupeptin, 0.086 mg/ml iodacetamide, 1 mM sodium orthovanadate) at 4°C for 30 min in rotation. Lysates were centrifuged for 20 min at 4°C at 13,000 rpm, and supernatants were stored at −80°C until use. EMSAs were performed as described (14). Briefly, binding reactions were prepared with 6 μg of nuclear extracts and 20,000 cpm ^{32}P-labeled probe in the presence of 2 μg of poly(dI:dC) in a final volume of 15 μl containing 1× binding buffer (12 mM HEPES (pH 7.9), 60 mM KCl, 5 mM $MgCl_2$, 0.12 mM EDTA, 0.3 mM PMSF, 0.3 mM DTT, 12% glycerol). The nuclear extracts were incubated for 8 min with poly(dI:dC) and then the radiolabeled probe was added and incubated for an additional 15 min at room temperature. Samples were loaded onto 4% acrylamide gel containing 5% glycerol and 0.25% TBE, and electrophoresed at 4°C. Band-shift gels were dried, and bands were visualized by autoradiography. For supershift experiments, following the binding reaction, 2 μl of anti-STAT5a and anti-STAT5b Abs were added and incubated for 30 min. The oligonucleotides used in the assay were 5′-end labeled using T_4 polynucleotide kinase (USB Corporation). The probe was synthesized by Genotek and corresponds to a GAS-like element from the promoter of the bovine β-casein gene (5′-AGATTTCTAGGAATTCAAATC-3′).

DNA damage susceptibility assay

To analyze macrophage susceptibility to various DNA-damaging agents, we treated the cells with etoposide (Tocris) and hydrogen peroxide (Sigma-Aldrich) at the concentrations indicated during 1 h and UV radiation (λ = 254 nm) at the energies indicated. Cells were washed and left in complete medium (DMEM + 10% FCS + 5 ng/ml M-CSF) for 5 days. Cells were counted by trypan blue exclusion, and cell growth was determined as the ratio of number of treated cells relative to number of control cells.

Determination of intracellular ROS

ROS levels were determined by FACS analysis. Briefly, cells were treated with 25 μM dichlorofluorescin diacetate (DCF-DA) for 20 min at 37°C, and fluorescence intensity was analyzed using an Epics XL flow cytometer (Coulter).

Telomere length quantification by real-time PCR

Telomere length was analyzed as described (15). Briefly, genomic DNA was isolated using the GFX genomic blood DNA purification kit (Amersham Biosciences), and real-time PCR was performed as in RNA expression analysis using 35 ng of DNA/well. Telomere length was calculated as the ratio of telomere repeat copy number to single copy gene (*36B4*) copy number (T/S ratio). This ratio should be proportional to the average telomere length. To confirm that the number of copies of the single copy gene per cell that was effectively PCR-amplified was the same in all individuals being studied, we quantified the relative ratio of *36B4* copies to *β-actin* copies. This ratio was ~1.0, indicating that equal copy numbers of *36B4* per cell were amplified in all DNA samples. Primer sequences and real-time conditions for telomere amplification were as described (15). Primer sequences for *36B4* and *β-actin* can be obtained upon request.

Cell surface staining

This assay was conducted using specific Abs and cytofluorometric analysis as described (12). Cells were incubated for 15 min with 1 μg/10^6 cells of anti-CD16/CD32 mAb to block Fc receptors. Then cells were incubated for 1 h with specific Abs at 4°C in the darkness. Cells were washed by centrifugation through an FCS cushion. Finally, they were fixed with PBS-2% paraformaldehyde. Stained cell suspensions were analyzed using an Epics XL flow cytometer (Coulter). The results were expressed as the mean ± SD.

Determination of ERK activity by in-gel kinase assay

ERK activity was analyzed as described (16) using 50–100 μg of total protein obtained and separated by 12.5% SDS-PAGE containing 0.1 mg/ml myelin basic protein (Sigma-Aldrich) as substrate co-polymerized in the gel. After several washes, denaturing, and renaturing, a phosphorylation assay was performed with 50 μM ATP and 100 μCi of [γ-^{32}P]ATP (GE Healthcare Biosciences).

Alkaline comet assay

Cells were treated with 250 μM H_2O_2 for 1 h and led to recover for the indicated times. Cells were then resuspended in 75 μl of 0.5% melting point agarose and led to solidify on clear slides precoated with 1% of normal agarose at 4°C. After solidification, the slides are placed in the lysis solution (100 mM EDTA, 2.5 M Trizma Base (pH 10), 1% Triton X-100 added just before use) for 1 h at 4°C. To express alkali-labile sites as single-strand breaks, the slides were incubated in alkaline electrophoresis buffer (1 mM EDTA, 300 mM NaOH, pH >13) for 20 min. Following alkaline unwinding, gels were electrophoresed under alkaline conditions (alkaline electrophoresis buffer) at 0.8–1.5 V/cm and 300 mA for 15 min. After electrophoresis, gels were neutralized with Tris buffer (pH 7.5), and comets were visualized by staining DNA with Hoescht. At least 50 comets per slide were scored. Images were captured with a Nikon Eclipse E800 fluorescence microscope and tail moment was quantified using the Soft imaging system (analySIS).

Analysis of oxidative DNA damage

Analysis of oxidative damage in specific gene sequences was performed as described (17). Briefly, genomic DNA was isolated using the GFX genomic blood DNA purification kit (Amersham Biosciences) in the presence of 20 μM 2,2,6,6-tetramethyl-1-piperidinyloxy, a free radical spin trap, to prevent in vitro oxidation. DNA (250 ng) was digested with FPG (formamidopyrimidine-DNA glycosylase) that selectively releases damaged bases from DNA, predominantly affecting the major oxidation product 8-oxoguanine. FPG creates a single-strand break at the apurinic site, rendering it resistant to PCR amplification. DNA damage was quantified as the ratio of intact PCR products in cleaved vs uncleaved DNA using real-time PCR with specific primers to exon 16 of *Stat5a* and exon 18 of *Stat5b* genes. The primers sequences can be obtained upon request.

Sequentiation

Genomic DNA from macrophages from three young and three aged mice was amplified using the Certamp enzyme mix (Biotools) and specific primers flanking from exon 15 to exon 17 of *Stat5a* gene (1085 bp). PCR products were purified and sequenced using the BigDye Terminator v3.1 cycle sequencing kit (Applied Biosystems) as described by the manufacturer in the 3730xl DNA analyzer (Applied Biosystems). Sequences were analyzed by the GeneWorks software (IntelliGenetics). The primers sequences can be obtained upon request.

Statistical analysis

Student's *t* test and one-way ANOVA test were used to calculate statistical differences between groups.

Results

Telomere shortening in aged macrophages

Telomere loss has been shown in several cell types during aging (18–21). In particular, cells of the immune system are highly susceptible to telomere attrition because of their high proliferative potential. Although mouse strains used in the laboratory have very long telomeres, recent studies have demonstrated that *Mus musculus* telomeres shorten with age in several stem cell compartments, such as skin, small intestine, cornea, testis and brain, thereby resulting in impaired stem cell functionality in old age (22). As expected the shortening of telomeres correlates with reduced telomerase activity. These data prompted us to analyze whether telomere shortening occurs in macrophages during aging. For this purpose, we used bone marrow-derived macrophages from young (6-wk-old) and aged (19–24-mo-old) mice. The production of macrophages in vitro prevents the presence of exogenous factors in young or aged mice that could modulate macrophage biology. We measured the relative telomere length of these cells by real-time PCR (15). Macrophages from aged mice had shorter telomeres than those from young mice (Fig. 1*A*). As a control, we determined the telomere length of macrophages from telomerase-deficient mice ($Terc^{-/-}$) (6-wk-old) of different generations (Fig. 1*B*). These mice show progressive telomere shortening in successive generations, with signs of premature aging between the third and sixth generations, depending on the genetic background (5). Telomere length differences were not significant between controls and G_1

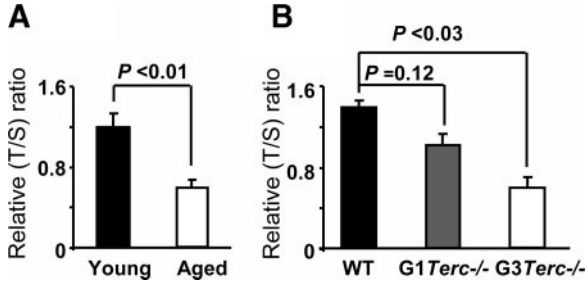

FIGURE 1. Telomeres shorten with age in macrophages. Telomere length was measured by real-time PCR in macrophages from young and aged mice ($n = 7$) (*A*), and in *Terc*-deficient mice and the corresponding controls ($n = 3$) (*B*). The ratio of relative telomere to single copy gene (*36B4*) amplification (T/S) was shown. The data represents the mean ± SEM.

$Terc^{-/-}$ macrophages, but a significant difference was found when we compared the controls and the G3 $Terc^{-/-}$ mice, as reported in other cell types (23). Noteworthy, no significant differences were found between telomere lengths from macrophages from young and control mice and the magnitude of telomere shortening during aging was similar to what we observed in macrophages from G3 $Terc^{-/-}$ mice (~50%). Thus, macrophage telomeres shorten during mouse aging, reaching the critical length observed in $Terc^{-/-}$ mice.

GM-CSF-dependent proliferation is impaired in macrophages from aged mice

Aging is associated with a decline in the proliferative capacity of cells, which has been shown to be related to the erosion of telomeres (24). Therefore, we decided to measure macrophage proliferation with two growth factors that are ligands for two different receptors. M-CSF induced the proliferation of macrophages from young and aged mice (Fig. 2, *A* and *B*). However, in the presence of GM-CSF, macrophages from aged mice did not proliferate even at saturating concentrations (10 ng/ml) (Fig. 2, *A* and *B*). A similar result was obtained when we used IL-3, which shares part of the receptor and the signal transduction with GM-CSF (Fig. 2*A*). These results were also confirmed by cell counting assays (Fig. 2*D*).

To characterize the proliferative response to GM-CSF, we analyzed the cell cycle progression of macrophages. After 18 h of growth factor deprivation, macrophages were arrested at G_1 phase. Treatment with M-CSF increased the proportion of both young and aged macrophages in the S phase, thereby indicating that these cells were progressing through the cell cycle (Fig. 2*C*). However, after GM-CSF stimulation, macrophages from aged mice were unable to progress through the cell cycle and remained arrested at G_1 phase (Fig. 2*C*). It is, in fact possible that the macrophages that respond to M-CSF and GM-CSF are two different cell populations, the GM-CSF responsive one being not present in old wild type. This possibility seems unrealistic because such macrophage populations, one with M-CSF receptors and another with GM-CSF receptors, has not been described. Together, these results demonstrate that GM-CSF-dependent proliferation is impaired in macrophages from aged mice because of a cell cycle blockade at the G_1 phase but not because of a defect in the machinery required for proliferation.

STAT5a phosphorylation and DNA-binding activity are reduced in macrophages from aged mice

We next studied the mechanism leading to GM-CSF-dependent impaired proliferation in aged macrophages. Macrophages from young and aged mice showed the same levels of the GM-CSF receptor expression of the α and βc subunit (β-chain common to IL-3R) (Fig. 3, *A* and *B*). These results indicate that the lack of

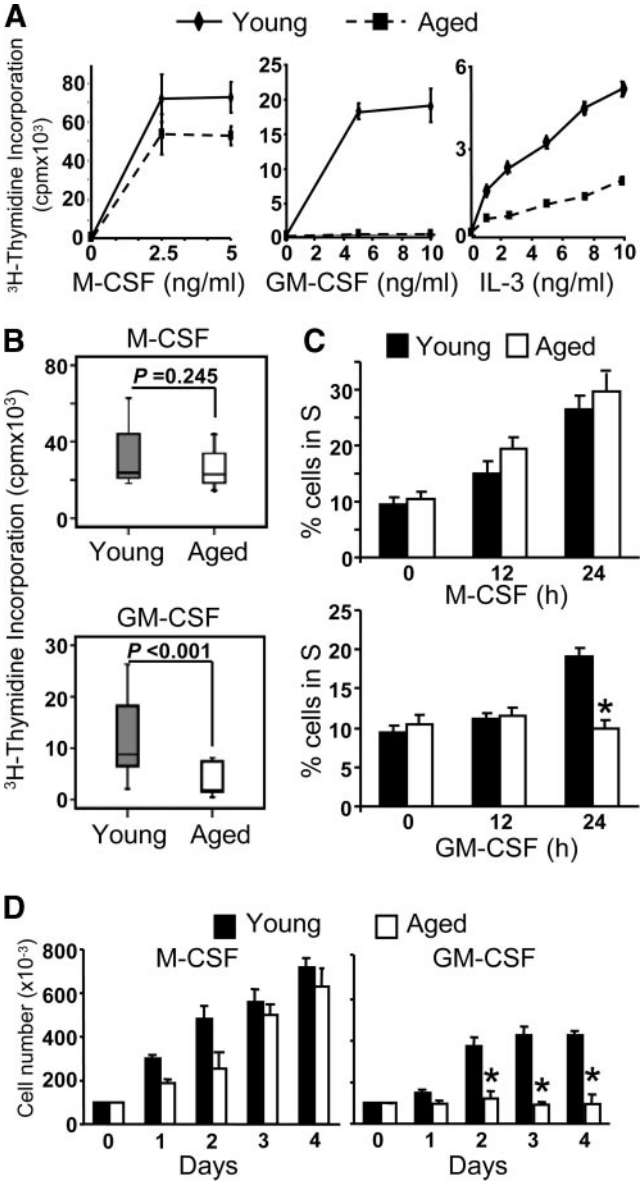

FIGURE 2. GM-CSF-dependent proliferation is impaired in macrophages from aged mice. *A*, M-CSF-, GM-CSF-, and IL-3-induced proliferation were determined by [^{3}H]thymidine incorporation in macrophages from young and aged mice. Macrophages were deprived of M-CSF for 18 h and then incubated for 24 h with different concentrations of M-CSF, GM-CSF, and IL-3. A representative experiment is shown. Each point was performed in triplicate and the results are shown as the mean ± SD. *B*, M-CSF- (5 ng/ml) and GM-CSF- (10 ng/ml) induced proliferation was determined by [^{3}H]thymidine incorporation in macrophages from young and aged mice ($n = 14$). *C*, Macrophages from young and aged mice were quiescent (control) or treated with saturating amounts of M-CSF (5 ng/ml) or GM-CSF (10 ng/ml), and their DNA content was measured by flow cytometry ($n = 6$). *D*, Macrophages from young and aged mice were led to grow in M-CSF (5 ng/ml) or GM-CSF (10 ng/ml) during 4 days, and cell counting was performed by an hemocytometer. ∗, $p < 0.01$ in relation to the corresponding control.

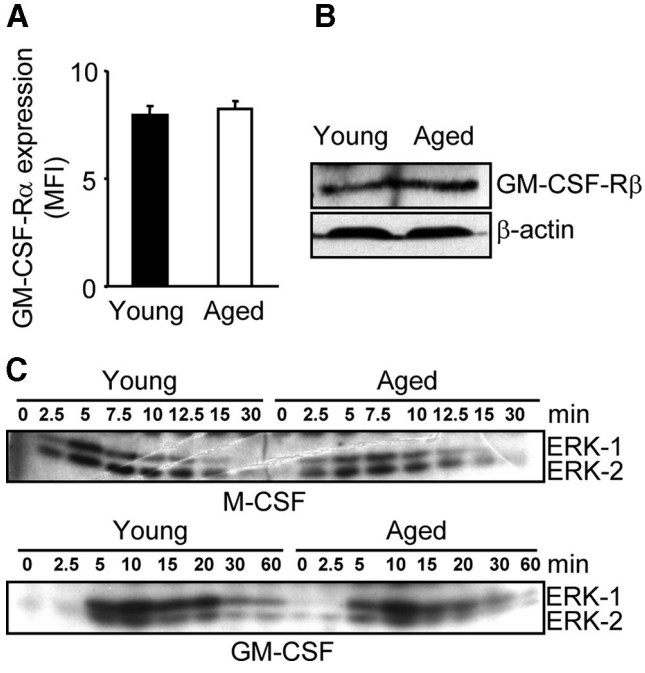

FIGURE 3. The GM-CSF receptor and the ERK response in aged macrophages was not impaired. *A*, GM-CSF receptor α-chain expression was determined by flow cytometry using a specific Ab. *B*, The expression of the β-chain of the GM-CSF-receptor was analyzed by Western blotting. *C*, ERK-1/2 activation was analyzed after treatment of macrophages with M-CSF (5 ng/ml) or GM-CSF (10 ng/ml) with an in-gel kinase assay as described in *Material and Methods*. These are representative figures of three independent experiments.

response to GM-CSF of macrophages from aged mice is not the result of impaired receptor expression. We then tested the effect of aging on the signaling pathways activated by the growth factors. M-CSF and GM-CSF require the activation of the ERK to induce macrophage proliferation (25). Both M-CSF- and GM-CSF-induced ERK activation showed similar levels and kinetics in macrophages from young and aged mice (Fig. 3*C*). In addition to ERK, the binding of GM-CSF with its receptor also induces the activation of the Janus kinase 2 (Jak2)/STAT5 pathway (26), which is involved in the proliferation of many cell types. In macrophages from young and aged mice, both STAT5a and STAT5b showed similar levels of mRNA and protein (Fig. 4, *A* and *B*). However, the GM-CSF-induced phosphorylation of STAT5 was reduced in macrophages from aged mice (Fig. 4*C*). Interestingly, although STAT5a and STAT5b proteins have 96% sequence identity (27), we found that only STAT5a phosphorylation was reduced in macrophages from aged mice (Fig. 4*D*).

Once phosphorylated, STAT5 dimerizes and translocates to the nucleus where it binds to DNA-specific sites and activates the transcription of target genes. Using a fragment of the *β-casein* promoter that contains a GAS box, we found that STAT5 bound to DNA in a similar manner in young and aged macrophages (Fig. 4*E*). Moreover, both STAT5a and STAT5b were present in the complexes, as shown by the supershift observed when specific Abs were added (Fig. 4*E*). Because STAT5a and STAT5b can bind to the same sequence, we repeated the assay but removing STAT5b from the nuclear extracts by immunoprecipitation. Using immunoblotting, we confirmed that STAT5b was not present in the nuclear extracts after immunoprecipitation (Fig. 4*F*). The EMSA with nuclear extracts in which STAT5b was absent showed a reduction in the DNA-binding activity of STAT5a in aged macrophages (Fig. 4*G*), thereby confirming impaired phosphorylation. Therefore, these results demonstrate the improper phosphorylation and DNA-binding activity of STAT5a in aged macrophages that may explain the lack of proliferation in response to GM-CSF, as has been shown in *Stat5a* knockout mice (28).

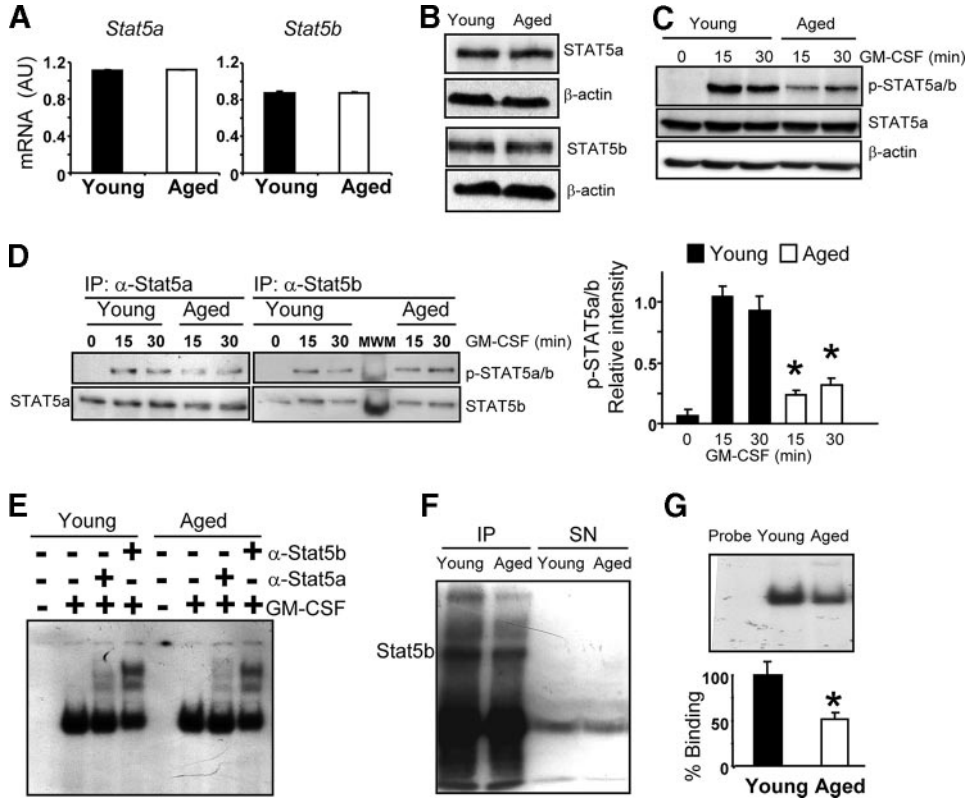

FIGURE 4. Phosphorylation and DNA-binding activity of STAT5a is reduced in aged macrophages. *A*, Expression of *Stat5* mRNAs was determined by real-time PCR. *B*, Protein expression of STAT5a and STAT5b was analyzed by Western blot. *C*, STAT5 phosphorylation was determined by Western blotting in a representative experiment. The graph represents the mean ± SEM of four independent experiments. *D*, Immunoprecipitation of STAT5a and STAT5b and immunoblotting with anti-phospho-STAT5a/b were conducted to analyze the phosphorylation of STAT5a and STAT5b. *E*, Nuclear extracts from macrophages from young and aged mice stimulated with GM-CSF (10 ng/ml) for 15 min were used to test the in vitro DNA-binding activity of STAT5 to a GAS-like element from the promoter of the bovine *β-casein* promoter. Specificity of shifted bands was corroborated by supershift experiments. *F*, STAT5b was immunoprecipitated from nuclear extracts of macrophages from young and aged mice. A Western blot was performed to confirm that Stat5b protein was in the immunoprecipitated (IP) fraction and the supernatant (SN) used for the EMSAs was free from STAT5b. *G*, DNA-binding activity of STAT5a was determined using STAT5b immunodepleted nuclear extracts from young and aged mice stimulated with GM-CSF (10 ng/ml) for 15 min. The graph represents the mean ± SEM of four independent experiments. ∗, $p < 0.01$ in relation to the corresponding control.

Macrophages from Terc$^{-/-}$ *mice show the same cellular defects as aged macrophages*

To determine the role of telomere shortening in the cellular defects observed in macrophages from aged mice, we used G3 *Terc*$^{-/-}$ mice. As in aged mice, bone marrow-derived macrophages from these mice showed impaired proliferation in response to GM-CSF but not to M-CSF (Fig. 5, *A* and *B*). To further study this finding, we used macrophages from the first generation of telomerase-deficient mice (G1 *Terc*$^{-/-}$). These mice lack telomerase activity but they do not show signs of premature aging. As telomeres shorten and chromosome fusions accumulate with increasing generations, these data indicate that in G_1 *Terc*$^{-/-}$ mice telomeres are not critically short (10, 23). In contrast to G3 *Terc*$^{-/-}$ mice, macrophages from G_1 *Terc*$^{-/-}$ mice had a normal proliferative response to GM-CSF (Fig. 5*A*). These results indicate that telomere shortening rather than loss of telomerase activity is involved in macrophage aging. Moreover, phosphorylation of STAT5a but not STAT5b was reduced in macrophages from G3 *Terc*$^{-/-}$ mice compared with the corresponding controls or G_1 *Terc*$^{-/-}$ mice (Fig. 5, *C* and *D*). These results reproduced those observed in macrophages from aged mice and suggest that either telomere shortening or the loss of telomerase activity is involved in the impaired proliferation of aged macrophages.

Macrophages from aged and G3 Terc$^{-/-}$ *mice show enhanced oxidative stress*

Oxidative stress has been proposed to be a major determinant of the aging process and has been related to the shortening of telomeres (24). To study how age-dependent telomere shortening affects macrophage proliferation, we focused on the macrophage response to this type of stress. Macrophages from aged mice showed decreased cell growth when treated with hydrogen peroxide. This observation suggests increased susceptibility to oxidative stress (Fig. 6*A*). However, no differences were observed with other DNA-damaging agents, such as etoposide or UV radiation, thereby confirming that the global response to stress is not impaired in macrophages from aged mice (Fig. 6*A*). In addition, aged macrophages showed enhanced levels of intracellular ROS (Fig. 6*B*). The magnitude of this increase was of the same level as that observed when we treated the cells with hydrogen peroxide. Furthermore, undifferentiated bone marrow cells from aged mice also showed increased levels of intracellular ROS (Fig. 6*C*), suggesting that the enhanced oxidative stress observed in aged macrophages is caused by alterations in their progenitor cells. In addition, the capacity of DNA repair after oxidative stress was also reduced in aged macrophages. Hydrogen peroxide treatment of macrophages from young mice caused an increase in the levels of γ-H2AX,

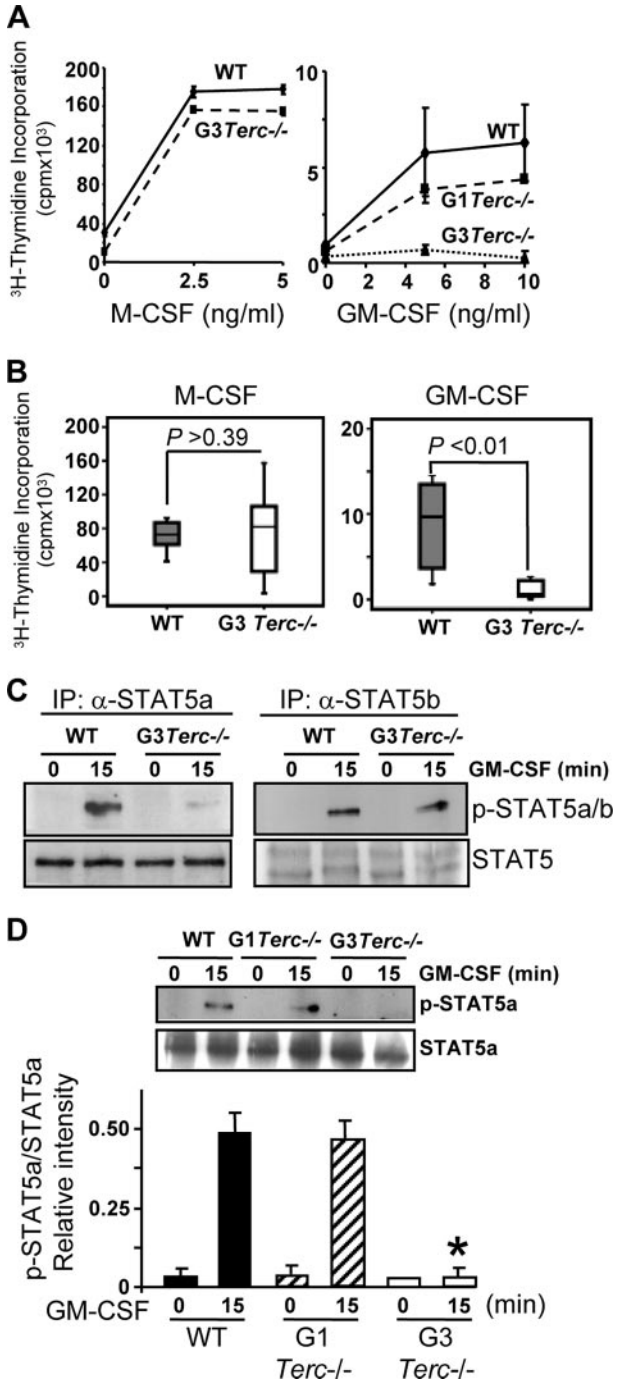

FIGURE 5. Macrophages from G3 *Terc*$^{-/-}$ mice show the same cellular defects observed in aged macrophages. *A*, M-CSF- and GM-CSF-induced proliferation was determined by [^{3}H]thymidine incorporation in macrophages from WT and G_1 or G3 *Terc*$^{-/-}$ mice. Macrophages were deprived of M-CSF for 18 h and then incubated for 24 h with different concentrations of M-CSF and GM-CSF. A representative experiment is shown. Each point was performed in triplicate and the results are shown as the mean ± SD. *B*, M-CSF- (5 ng/ml) and GM-CSF- (10 ng/ml) induced proliferation was determined by [^{3}H]thymidine incorporation in macrophages from WT and G3 *Terc*$^{-/-}$ mice ($n = 7$). *C*, Immunoprecipitation of STAT5a and STAT5b and immunoblotting with anti-phospho-STAT5a/b were conducted to analyze the phosphorylation of STAT5a and STAT5b. These figures are representative of at least three independent experiments. *D*, Immunoprecipitation of STAT5a and immunoblotting with anti-phospho-STAT5a/b were conducted to analyze the phosphorylation of STAT5a in macrophages from WT, G_1, and G3 *Terc*$^{-/-}$ mice. The data is representative of three independent experiments. The graph represents the mean ± SEM of four independent experiments. ∗, $p < 0.01$ in relation to the corresponding control.

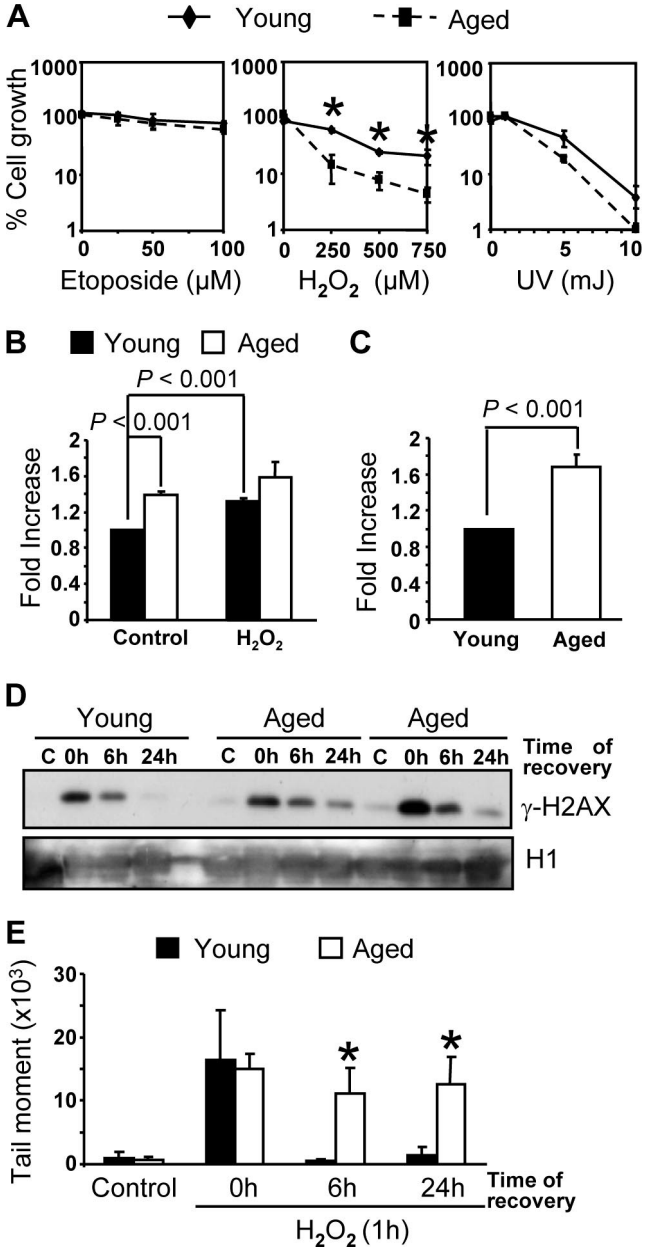

FIGURE 6. Enhanced oxidative stress in aged macrophages. *A*, Macrophages from young and aged mice were treated with several DNA-damaging agents and led to recover for 5 days. Cell growth was determined as the ratio of the number of treated cells relative to the number of control cells. The data represents the mean ± SEM of four independent experiments. Intracellular levels of ROS were quantified in macrophages (*B*) and bone marrow cells (*C*) by staining with the ROS-specific dye DCF-DA. In *B*, hydrogen peroxide was added at 250 μM for 1 h as a positive control. The data represents the mean ± SEM of three independent experiments. *D*, Macrophages from young and aged mice were treated with hydrogen peroxide (250 μM) for 1 h; the cells were washed and led to recover for 6 and 24 h. DNA damage was determined by γ-H2AX immunoblotting (*c*, untreated cells). This figure is representative of three independent experiments. *E*, Alkaline Comet assay was performed to analyze DNA damage after oxidative stress in macrophages from young and aged mice. Quantification was done using the tail moment calculation. This figure is representative of three independent experiments. ∗, $p < 0.01$ in relation to the corresponding control.

which returned to basal levels after 24 h of recovery (Fig. 6*D*). However, macrophages from aged mice showed sustained levels of γ-H2AX, thereby indicating a decreased response to oxidative

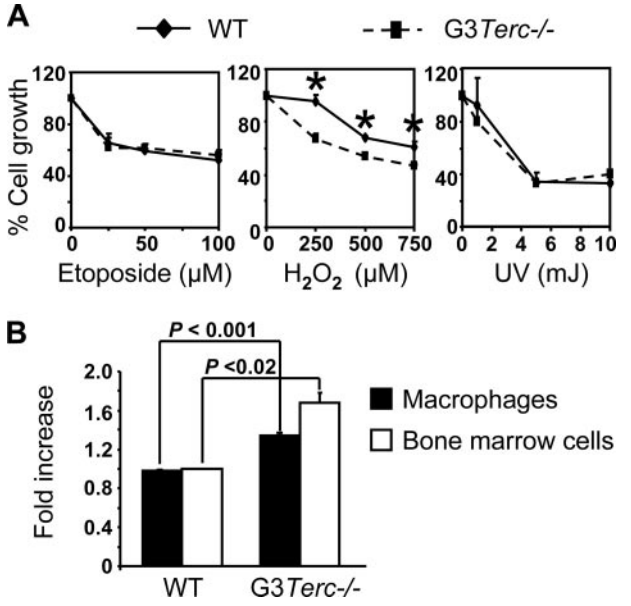

FIGURE 7. Enhanced oxidative stress in G3 $Terc^{-/-}$ mice. *A*, Macrophages from WT and G3 $Terc^{-/-}$ mice were treated with distinct DNA-damaging agents and left to recover for 5 days. Cell growth was determined as the ratio of the number of treated cells relative to the number of control cells. The data represents the mean ± SEM of four independent experiments; ∗, $p < 0.01$ in relation to the corresponding control. *B*, Intracellular levels of ROS were quantified in macrophages and bone marrow cells by staining with the ROS-specific dye DCF-DA. The data represents the mean ± SEM ($n = 4$).

stress. Alkaline comet assay, which detects DNA single-strand breaks, further confirmed this reduced DNA repair capacity (Fig. 6*E*). Together, these results demonstrate that macrophages from aged mice suffer enhanced oxidative stress.

In addition to aged mice, macrophages from G3 $Terc^{-/-}$ mice also showed increased susceptibility to oxidative stress but not to other types of stress factors, compared with control mice (Fig. 7*A*). Strikingly, intracellular levels of ROS were also increased in macrophages and bone marrow cells (Fig. 7B) from G3 $Terc^{-/-}$ mice, thereby linking the two models again, the aged and telomerase-deficient mice.

STAT5a oxidation is reduced in macrophages from aged and G3 Terc$^{-/-}$ *mice*

Next, we addressed whether oxidative stress is related to the reduction in STAT5a phosphorylation in macrophages from aged and G3 $Terc^{-/-}$ mice. Our first hypothesis was that oxidative stress leads to a mutation in the genomic DNA of STAT5a. Although *STAT5a* and *STAT5b* are coded by two distinct genes, they are highly homologous proteins (96% sequence identity) (27), differing only in their COOH-terminal transactivation domain, which contains a tyrosine residue that is phosphorylated in response to GM-CSF (29). We sequenced the genomic DNA from three young and three aged mice using primers flanking the exons containing this domain in *STAT5a* (exon 16) but we did not find any difference between macrophages from these two groups. However, oxidative damage may also cause base oxidation, which is not detected by the sequencing technique. To examine this possibility, we digested genomic DNA with formamidopyrimidine-DNA glycosylase. This enzyme cleaves the oxidized base, thereby generating an AP site that prevents PCR amplification. We then quantified the DNA oxidation by real-time PCR. No difference between young and aged macrophages in the base oxidation in this exon was observed (Fig. 8*A*).

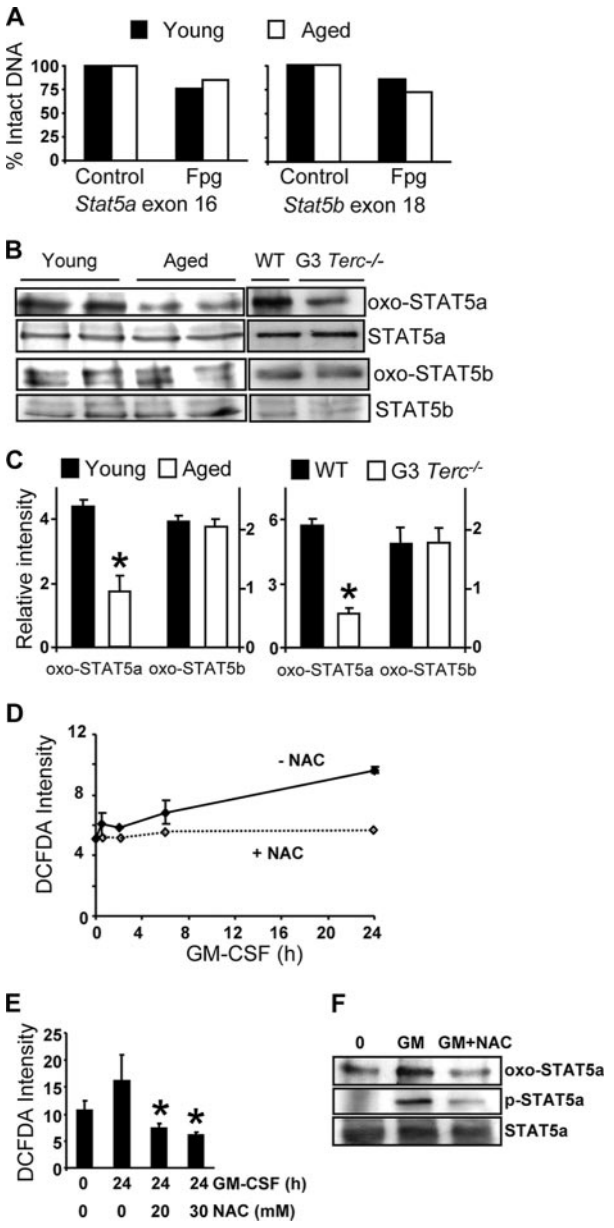

FIGURE 8. Decreased Stat5a oxidation in macrophages from aged and G3 $Terc^{-/-}$ mice. *A*, Genomic DNA was extracted from young and aged macrophages and digested with formamidopyrimidine-DNA glycosylase (Fpg). Quantification of oxidative DNA damage was performed by real-time PCR of exon 16 of *Stat5a* and exon 18 of *Stat5b*. These figures are representative of four independent experiments. *B*, STAT5a and STAT5b were immunoprecipitated from protein extracts from macrophages from young, aged, WT, and G3 $Terc^{-/-}$ mice stimulated with GM-CSF (10 ng/ml) and oxidation of Stat5 proteins was determined using an Ab recognizing the carbonyl groups introduced into proteins by oxidative reactions. *C*, The graphs represent the mean ± SEM of four independent experiments. *D*, Macrophages from young mice were stimulated with 10 ng/ml GM-CSF in the presence or absence of 20 mM NAC for the indicated times, and intracellular ROS levels were analyzed by DCF-DA staining. Each point was performed in triplicate and the results are shown as the mean ± SD. *E*, Macrophages from young mice were treated with 10 ng/ml GM-CSF for 24 h in the presence or absence of NAC at the concentrations indicated. ROS levels were measured by DCF-DA staining. The data represents the mean ± SEM of four independent experiments. *F*, STAT5a was immunoprecipitated from protein extracts from macrophages treated with 10 ng/ml GM-CSF in the presence or absence of 20 mM NAC, and oxidation of the protein was determined. This figure is representative of at least three independent experiments. ∗, $p < 0.01$ in relation to the corresponding control.

In addition to DNA, oxidative stress can directly inflict damage on proteins and lipids (30). Therefore we analyzed the oxidation status of STAT5 proteins by immunodetecting the carbonyl groups introduced into protein side chains as a consequence of oxidation. Surprisingly, STAT5a was less oxidized in macrophages from aged mice, whereas no differences were observed in STAT5b (Fig. 8, *B* and *C*). Moreover, macrophages from G3 *Terc*$^{-/-}$ mice also showed impaired oxidation of STAT5a but not STAT5b (Fig. 8, *B* and *C*). These results suggest that the increased levels of oxidative stress in aged and G3 *Terc*$^{-/-}$ macrophages cause a reduction in the oxidation of STAT5a.

STAT5a oxidation is required for this signal transducer to be phosphorylated

Because STAT5a oxidation and phosphorylation were reduced in macrophages from aged and G3 *Terc*$^{-/-}$ mice, we addressed whether these two reactions were related. It has been reported that hematopoietic cytokines induce an increase in intracellular ROS levels, thereby promoting the phosphorylation of several proteins, including STAT5 (31, 32). After the addition of GM-CSF, ROS production showed a gradual increase from 30 min to 24 h (Fig. 8*D*). The addition of the ROS scavenger *N*-acetylcysteine (NAC) blocked the effect of GM-CSF (Fig. 8*D*). Interestingly, stimulation of macrophages with GM-CSF induced STAT5a oxidation (Fig. 8*E*) and the treatment of these cells with NAC, which blocked this oxidation, also inhibited the phosphorylation of STAT5a (Fig. 8*F*). These results suggest that STAT5a oxidation is required for its phosphorylation, thereby confirming that the reduced phosphorylation of STAT5a observed in macrophages from aged and G3 *Terc*$^{-/-}$ mice is due to its impaired oxidation.

Discussion

The results presented suggest that the loss of telomeric sequences during aging is responsible for the enhanced oxidative stress, the impaired oxidation and phosphorylation of STAT5a and the reduced proliferation of macrophages. This study provides one of the few reports that telomere shortening occurs in the mouse strain *Mus musculus*, which has very long telomeres. In addition, our observation that the telomere length of macrophages from aged and G3 *Terc*$^{-/-}$ mice was very similar indicates that normal aging leads to short telomeres, thereby resulting in impaired proliferation.

In this study, we used bone marrow-derived macrophages differentiated in vitro. Thus, the variations in telomere length in these cells during aging may reflect changes in telomere length in hematopoietic progenitor cells. In fact, hematopoietic stem cells show telomere shortening during in vitro culture and in vivo aging (21, 33, 34). Hematopoietic stem cells derived from humans and mice lose telomeric DNA with age despite the presence of detectable telomerase activity (21, 35). Moreover, telomeres shorten with age in several mouse stem cell compartments, including skin, small intestine, cornea, testis and brain (22).

In addition to telomere shortening, we have shown that macrophages from aged mice suffer enhanced oxidative stress. This kind of stress has been associated with telomere shortening as reflected by the observation that cells with enhanced oxidative stress have shorter telomeres (24, 36). However, our finding that G3 *Terc*$^{-/-}$ mice also have an enhanced oxidative stress points to telomere shortening as the cause of the enhanced oxidative stress in macrophages. These results correlate with those observed in mouse embryonic fibroblasts derived from *Terc*$^{-/-}$ mice, which also show increased levels of ROS (37). In fact, telomerase deficiency reduces catalase activity that determines a redox imbalance (38). Furthermore, it has been shown that cells overexpressing telomerase accumulate lower concentrations of peroxides (39). Undifferentiated bone marrow cells from aged and G3 *Terc*$^{-/-}$ mice also show an increase in intracellular ROS, thereby further supporting the hypothesis that macrophage aging is due to an intrinsic alteration in their progenitor cells. Recently it has been reported that in the absence of telomeres there is a repression of genes located within 10 kb (40). Although in mice, catalase is located in the central area of the chromosome 2, we cannot exclude that telomeres are required to regulate transcription factors or other elements necessary for catalase expression.

Telomere shortening is associated with the impaired proliferation of many cell types, including those of the immune system (6, 7). Surprisingly, in our studies only GM-CSF- but not M-CSF-dependent proliferation of macrophages was affected by aging. This is attributed to a reduction of STAT5a oxidation, which leads to impaired phosphorylation. Notably, it has been described that STAT5 phosphorylation is reduced during aging in T (41) and B cells (42) and neutrophils (43), thereby leading to a number of functional alterations. Aging is associated with a reduction in B and T cell numbers (44), suggesting that impaired STAT5 phosphorylation is a general effect of aging involved in many aspects of immunosenescence. G3 *Terc*$^{-/-}$ but not G_1 *Terc*$^{-/-}$ macrophages showed the same cellular defects as those observed in aged mice. These results indicate that telomere attrition and oxidative stress cause a decrease in the oxidation and phosphorylation of STAT5a and, therefore, impaired proliferation of macrophages. However, the precise mechanism linking enhanced oxidative stress and reduced STAT5a oxidation and phosphorylation remains to be elucidated. One may think that oxidative stress could affect the activity of tyrosine phosphatases. However, reversible oxidation of Cys residues on these phosphatases leads to their inhibition (45, 46), which would result in an increase of the amount of phospho-STAT5a, instead of the reduced levels of phosphorylation that we observe under oxidative stress conditions. The generation of ROS by GM-CSF stimulation may be through activation of NADPH oxidase, as observed for other cytokines (47, 48). Thus, it is possible that a permanent increase in oxidative stress in aged macrophages may cause a redox-dependent modification in NADPH oxidase, leading to an impaired production of ROS and STAT5a phosphorylation. However, further assays are required to prove this hypothesis.

In summary, in this study we describe that macrophage telomeres shorten during mouse aging, thereby leading to impaired GM-CSF-dependent proliferation of these cells. In addition, we present data about the molecular mechanisms involved in this process. GM-CSF plays a crucial role during inflammation. Proinflammatory functions of GM-CSF include the recruitment, activation, enhanced survival, proliferation and adhesion of neutrophils and macrophages (49). Therefore, it is likely that GM-CSF has a central role in regulating macrophage proliferation at sites of inflammation (50, 51). Thus, impaired response of macrophages to GM-CSF during aging may have relevant consequences on inflammatory reactions and on host defenses against a broad spectrum of invading organisms. In this regard, it is important to note that human aging is generally accompanied by elevated systemic inflammatory conditions (52) and that macrophages play a key role during this process.

Acknowledgments

We thank Tanya Yates for editing the manuscript. The help of Javier Gonzalez-Linares and Joaquín de Lafuente from the Toxicology Unit at the Parc Cientific of Barcelona in the alkaline comet assay is acknowledged.

Disclosures

The authors have no financial conflict of interest.

References

1. Miller, R. A. 1996. The aging immune system: primer and prospectus. *Science* 273: 70–74.
2. Plowden, J., M. Renshaw-Hoelscher, C. Engleman, J. Katz, and S. Sambhara. 2004. Innate immunity in aging: impact on macrophage function. *Aging Cell* 3: 161–167.
3. Blackburn, E. H. 2001. Switching and signaling at the telomere. *Cell* 106: 661–673.
4. Iwama, H., K. Ohyashiki, J. H. Ohyashiki, S. Hayashi, N. Yahata, K. Ando, K. Toyama, A. Hoshika, M. Takasaki, M. Mori, and J. W. Shay. 1998. Telomeric length and telomerase activity vary with age in peripheral blood cells obtained from normal individuals. *Hum. Genet.* 102: 397–402.
5. Samper, E., P. Fernandez, R. Eguia, L. Martin-Rivera, A. Bernad, M. A. Blasco, and M. Aracil. 2002. Long-term repopulating ability of telomerase-deficient murine hematopoietic stem cells. *Blood* 99: 2767–2775.
6. Blasco, M. A. 2002. Immunosenescence phenotypes in the telomerase knockout mouse. *Springer Semin. Immunopathol.* 24: 75–85.
7. Hodes, R. J., K. S. Hathcock, and N. P. Weng. 2002. Telomeres in T and B cells. *Nat. Rev. Immunol.* 2: 699–706.
8. Herrero, C., L. Marques, J. Lloberas, and A. Celada. 2001. IFN-γ-dependent transcription of MHC class II IA is impaired in macrophages from aged mice. *J. Clin. Invest.* 107: 485–493.
9. Celada, A., P. W. Gray, E. Rinderknecht, and R. D. Schreiber. 1984. Evidence for a γ-interferon receptor that regulates macrophage tumoricidal activity. *J. Exp. Med.* 160: 55–74.
10. Blasco, M. A., H. W. Lee, M. P. Hande, E. Samper, P. M. Lansdorp, R. A. DePinho, and C. W. Greider. 1997. Telomere shortening and tumor formation by mouse cells lacking telomerase RNA. *Cell* 91: 25–34.
11. Celada, A., F. E. Borras, C. Soler, J. Lloberas, M. Klemsz, C. van Beveren, S. McKercher, and R. A. Maki. 1996. The transcription factor PU. 1 is involved in macrophage proliferation. *J. Exp. Med.* 184: 61–69.
12. Xaus, J., M. Cardo, A. F. Valledor, C. Soler, J. Lloberas, and A. Celada. 1999. Interferon γ induces the expression of p21waf-1 and arrests macrophage cell cycle, preventing induction of apoptosis. *Immunity* 11: 103–113.
13. Valledor, A. F., J. Xaus, L. Marques, and A. Celada. 1999. Macrophage colony-stimulating factor induces the expression of mitogen-activated protein kinase phosphatase-1 through a protein kinase C-dependent pathway. *J. Immunol.* 163: 2452–2462.
14. Casals, C., M. Barrachina, M. Serra, J. Lloberas, and A. Celada. 2007. Lipopolysaccharide up-regulates MHC class II expression on dendritic cells through an AP-1 enhancer without affecting the levels of CIITA. *J. Immunol.* 178: 6307–6315.
15. Cawthon, R. M. 2002. Telomere measurement by quantitative PCR. *Nucleic Acids Res.* 30: e47.
16. Valledor, A. F., J. Xaus, M. Comalada, C. Soler, and A. Celada. 2000. Protein kinase C ϵ is required for the induction of mitogen-activated protein kinase phosphatase-1 in lipopolysaccharide-stimulated macrophages. *J. Immunol.* 164: 29–37.
17. Lu, T., Y. Pan, S. Y. Kao, C. Li, I. Kohane, J. Chan, and B. A. Yankner. 2004. Gene regulation and DNA damage in the ageing human brain. *Nature* 429: 883–891.
18. Canela, A., E. Vera, P. Klatt, and M. A. Blasco. 2007. High-throughput telomere length quantification by FISH and its application to human population studies. *Proc. Natl. Acad. Sci. USA* 104: 5300–5305.
19. Harley, C. B., A. B. Futcher, and C. W. Greider. 1990. Telomeres shorten during ageing of human fibroblasts. *Nature* 345: 458–460.
20. Rufer, N., W. Dragowska, G. Thornbury, E. Roosnek, and P. M. Lansdorp. 1998. Telomere length dynamics in human lymphocyte subpopulations measured by flow cytometry. *Nat. Biotechnol.* 16: 743–747.
21. Vaziri, H., W. Dragowska, R. C. Allsopp, T. E. Thomas, C. B. Harley, and P. M. Lansdorp. 1994. Evidence for a mitotic clock in human hematopoietic stem cells: loss of telomeric DNA with age. *Proc. Natl. Acad. Sci. USA* 91: 9857–9860.
22. Flores, I., A. Canela, E. Vera, A. Tejera, G. Cotsarelis, and M. A. Blasco. 2008. The longest telomeres: a general signature of adult stem cell compartments. *Genes Dev.* 22: 654–667.
23. Herrera, E., E. Samper, J. Martin-Caballero, J. M. Flores, H. W. Lee, and M. A. Blasco. 1999. Disease states associated with telomerase deficiency appear earlier in mice with short telomeres. *EMBO J.* 18: 2950–2960.
24. von Zglinicki, T. 2002. Oxidative stress shortens telomeres. *Trends Biochem. Sci.* 27: 339–344.
25. Valledor, A. F., M. Comalada, J. Xaus, and A. Celada. 2000. The differential time-course of extracellular-regulated kinase activity correlates with the macrophage response toward proliferation or activation. *J. Biol. Chem.* 275: 7403–7409.
26. de Groot, R. P., P. J. Coffer, and L. Koenderman. 1998. Regulation of proliferation, differentiation and survival by the IL-3/IL-5/GM-CSF receptor family. *Cell Signal* 10: 619–628.
27. Hou, J., U. Schindler, W. J. Henzel, S. C. Wong, and S. L. McKnight. 1995. Identification and purification of human Stat proteins activated in response to interleukin-2. *Immunity* 2: 321–329.
28. Feldman, G. M., L. A. Rosenthal, X. Liu, M. P. Hayes, A. Wynshaw-Boris, W. J. Leonard, L. Hennighausen, and D. S. Finbloom. 1997. STAT5A-deficient mice demonstrate a defect in granulocyte-macrophage colony-stimulating factor-induced proliferation and gene expression. *Blood* 90: 1768–1776.
29. Moriggl, R., D. J. Topham, S. Teglund, V. Sexl, C. McKay, D. Wang, A. Hoffmeyer, J. van Deursen, M. Y. Sangster, K. D. Bunting, et al. 1999. Stat5 is required for IL-2-induced cell cycle progression of peripheral T cells. *Immunity* 10: 249–259.
30. Blumberg, J. 2004. Use of biomarkers of oxidative stress in research studies. *J. Nutr.* 134: 3188S–3189S.
31. Iiyama, M., K. Kakihana, T. Kurosu, and O. Miura. 2006. Reactive oxygen species generated by hematopoietic cytokines play roles in activation of receptor-mediated signaling and in cell cycle progression. *Cell Signal* 18: 174–182.
32. Sattler, M., T. Winkler, S. Verma, C. H. Byrne, G. Shrikhande, R. Salgia, and J. D. Griffin. 1999. Hematopoietic growth factors signal through the formation of reactive oxygen species. *Blood* 93: 2928–2935.
33. Zimmermann, S., S. Glaser, R. Ketteler, C. F. Waller, U. Klingmuller, and U. M. Martens. 2004. Effects of telomerase modulation in human hematopoietic progenitor cells. *Stem Cells* 22: 741–749.
34. Engelhardt, M., R. Kumar, J. Albanell, R. Pettengell, W. Han, and M. A. Moore. 1997. Telomerase regulation, cell cycle, and telomere stability in primitive hematopoietic cells. *Blood* 90: 182–193.
35. Allsopp, R. C., S. Cheshier, and I. L. Weissman. 2001. Telomere shortening accompanies increased cell cycle activity during serial transplantation of hematopoietic stem cells. *J. Exp. Med.* 193: 917–924.
36. Tchirkov, A., and P. M. Lansdorp. 2003. Role of oxidative stress in telomere shortening in cultured fibroblasts from normal individuals and patients with ataxia-telangiectasia. *Hum. Mol. Genet.* 12: 227–232.
37. Perez-Rivero, G., M. P. Ruiz-Torres, J. V. Rivas-Elena, M. Jerkic, M. L. Diez-Marques, J. M. Lopez-Novoa, M. A. Blasco, and D. Rodriguez-Puyol. 2006. Mice deficient in telomerase activity develop hypertension because of an excess of endothelin production. *Circulation* 114: 309–317.
38. Perez-Rivero, G., M. P. Ruiz-Torres, M. L. Diez-Marques, A. Canela, J. M. Lopez-Novoa, M. Rodriguez-Puyol, M. A. Blasco, and D. Rodriguez-Puyol. 2008. Telomerase deficiency promotes oxidative stress by reducing catalase activity. *Free Radic. Biol. Med.* 45: 1243–1251.
39. Armstrong, L., G. Saretzki, H. Peters, I. Wappler, J. Evans, N. Hole, T. von Zglinicki, and M. Lako. 2005. Overexpression of telomerase confers growth advantage, stress resistance, and enhanced differentiation of ESCs toward the hematopoietic lineage. *Stem Cells* 23: 516–529.
40. Yang, X., L. M. Figueiredo, A. Espinal, E. Okubo, and B. Li. 2009. RAP1 is essential for silencing telomeric variant surface glycoprotein genes in Trypanosoma brucei. *Cell* 137: 99–109.
41. Fulop, T., Jr., N. Douziech, A. C. Goulet, S. Desgeorges, A. Linteau, G. Lacombe, and G. Dupuis. 2001. Cyclodextrin modulation of T lymphocyte signal transduction with aging. *Mech. Ageing Dev.* 122: 1413–1430.
42. Riley, R. L., E. Van der Put, A. M. King, D. Frasca, and B. B. Blomberg. 2005. Deficient B lymphopoiesis in murine senescence: potential roles for dysregulation of E2A, Pax-5, and STAT5. *Semin. Immunol.* 17: 330–336.
43. Fortin, C. F., A. Larbi, G. Dupuis, O. Lesur, and T. Fulop, Jr. 2007. GM-CSF activates the Jak/STAT pathway to rescue polymorphonuclear neutrophils from spontaneous apoptosis in young but not elderly individuals. *Biogerontology* 8: 173–187.
44. Hakim, F. T., and R. E. Gress. 2007. Immunosenescence: deficits in adaptive immunity in the elderly. *Tissue Antigens* 70: 179–189.
45. Salmeen, A., and D. Barford. 2005. Functions and mechanisms of redox regulation of cysteine-based phosphatases. *Antioxid. Redox. Signal* 7: 560–577.
46. Rhee, S. G., Y. S. Bae, S. R. Lee, and J. Kwon. 2000. Hydrogen peroxide: a key messenger that modulates protein phosphorylation through cysteine oxidation. *Sci. STKE* 2000: PE1.
47. Bae, Y. S., J. Y. Sung, O. S. Kim, Y. J. Kim, K. C. Hur, A. Kazlauskas, and S. G. Rhee. 2000. Platelet-derived growth factor-induced H_2O_2 production requires the activation of phosphatidylinositol 3-kinase. *J. Biol. Chem.* 275: 10527–10531.
48. Chiarugi, P., and P. Cirri. 2003. Redox regulation of protein tyrosine phosphatases during receptor tyrosine kinase signal transduction. *Trends Biochem. Sci.* 28: 509–514.
49. Hamilton, J. A. 2002. GM-CSF in inflammation and autoimmunity. *Trends Immunol.* 23: 403–408.
50. Bozinovski, S., J. E. Jones, R. Vlahos, J. A. Hamilton, and G. P. Anderson. 2002. Granulocyte/macrophage-colony-stimulating factor (GM-CSF) regulates lung innate immunity to lipopolysaccharide through Akt/Erk activation of NFkappa B and AP-1 in vivo. *J. Biol. Chem.* 277: 42808–42814.
51. Bitterman, P. B., L. E. Saltzman, S. Adelberg, V. J. Ferrans, and R. G. Crystal. 1984. Alveolar macrophage replication. One mechanism for the expansion of the mononuclear phagocyte population in the chronically inflamed lung. *J. Clin. Invest.* 74: 460–469.
52. Franceschi, C., M. Bonafe, S. Valensin, F. Olivieri, M. De Luca, E. Ottaviani, and G. De Benedictis. 2000. Inflamm-aging. An evolutionary perspective on immunosenescence. *Ann. NY Acad. Sci.* 908: 244–254.